

Structural, Magnetic, and Magnetocaloric Properties of $\text{La}_{1-x}\text{Bi}_x\text{MnO}_3$ ($x = 0.01, 0.03, 0.06, 0.1, 0.2$) Compounds

VELI SERKAN KOLAT, SELCUK ATALAY, TEKIN IZGI, HUSEYIN GENCER,
and NEVZAT BAYRI

Bi-doped lanthanum manganites with chemical composition of $\text{La}_{1-x}\text{Bi}_x\text{MnO}_3$ ($x = 0.01, 0.03, 0.06, 0.1,$ and 0.2) were prepared by a standard solid-state process. Magnetic and magnetocaloric properties of the samples were investigated in detail. X-ray diffraction measurement showed that the sample crystallized in the single phase of orthorhombic structure. It was found that the magnetization, Curie temperature, and the maximum value of magnetic entropy change decrease with increasing Bi content. The decrease in magnetic entropy change was attributed to the decrease in saturation magnetization and a change of the nature of the phase transition from first order to second order with increasing Bi content.

DOI: 10.1007/s11661-015-2839-y

© The Minerals, Metals & Materials Society and ASM International 2015

I. INTRODUCTION

THE mixed-valence perovskite manganites of type $\text{La}_{1-x}\text{A}_x\text{MnO}_3$ ($\text{A} = \text{Ca}, \text{Sr}, \text{Pb}, \text{Ba}$) have recently been studied in detail due to the colossal magnetoresistance (CMR) and magnetocaloric (MC) properties displayed by some compounds of that family.^[1,2] The cause of increasing interest in the perovskite manganites is because these materials have great potential in technological applications related to the CMR and MC such as magnetic sensors, computer memory systems, and magnetic refrigerants in magnetic refrigeration technology.^[3] They have also many fascinating magnetic and electronic properties such as orbital and charge ordering, structural and magnetic phase separation, and insulator-metal and antiferromagnetic-ferromagnetic phase transition.^[4] The undoped parent LaMnO_3 is an antiferromagnetic insulator. When the substitution of a divalent rare-earth metal ($\text{Ca}^{2+}, \text{Sr}^{2+}, \text{Ba}^{2+}$) for La^{3+} , some of the Mn^{3+} ions transformed to Mn^{4+} ions (which is called as mixed-valence state), results in the transition from an antiferromagnetic insulating state to a ferromagnetic metallic state. The origin of ferromagnetism and antiferromagnetism, as well as the transport properties in these systems, has been well explained by double-exchange (DE) interaction (between Mn^{3+} and Mn^{4+} ions) and super-exchange (SE) interaction (between Mn^{3+} and $\text{Mn}^{3+(4+)}$ ions).^[5] However, DE interactions promoting FM spin ordering and SE interactions favor an AFM spin arrangement. The resultant magnetic and transport properties of these systems are determined by competition between DE and SE interaction. All the previous studies have shown that

ferromagnetic phase in manganites was observed in compounds having only mixed-valence state.

On the other hand, among the all other usual perovskite-type manganites, compound BiMnO_3 exhibits a very different structure and properties. While LaMnO_3 has an antiferromagnetic ordering, BiMnO_3 is characterized by ferromagnetic ordering with a Curie temperature of 105 K to 110 K (-168°C to -163°C).^[6-9] Interestingly, BiMnO_3 is the only reported manganite showing ferromagnetic order even if only a $3+$ valence has on the Mn site. Although there is no any Mn^{4+} ion (in this case DE interaction could not exist), the origin of ferromagnetism in Bi-doped manganites is still not clear. Although there was a large amount of work,^[7,10-19] some of the results are still contradictory. The fundamental magnetic characteristics of Bi-doped manganites have not been clarified yet. The interesting point here is what causes this change in magnetic and transport properties, despite the very similar ionic radii and oxidation states of La^{3+} and Bi^{3+} ions. All the above-mentioned properties make this compound very special in comparison to other manganites perovskites. In recent studies, it has been shown that the MnO_6 octahedra in Bi-doped manganites are fairly distorted. Consequently, the replacement of La by Bi causes an increase of the Mn-O-Mn distortion. It has been concluded that the strongly polarized Bi lone-pair electrons are responsible for the heavily distorted structure.^[20-22] Khomchenko *et al.*^[15] have concluded that the existence of ferromagnetism in Bi-doped LaMnO_3 is considered to be caused by specific ordering of the d_{z^2} orbitals of the Mn^{3+} ions. The relative spatial position of the d_{z^2} orbitals is so that two-thirds of the total numbers of exchange interactions are positive and that the resulting structure is ferromagnetic.^[9,23]

Interestingly, while the electrical and magnetic properties of Bi-doped $\text{La}_{1-x}\text{Bi}_x\text{MnO}_3$ compounds have been studied fairly, there has been no report about magnetocaloric effect of Bi-doped $\text{La}_{1-x}\text{Bi}_x\text{MnO}_3$ compounds. Therefore, in this work, the effect of Bi doping

VELI SERKAN KOLAT, SELCUK ATALAY, TEKIN IZGI, HUSEYIN GENCER, and NEVZAT BAYRI, Lecturers in Physics, are with the Physics Department, Science and Arts Faculty, Inonu University, 44280 Malatya, Turkey. Contact e-mails: satalay@inonu.edu.tr; selcuk.atalay@inonu.edu.tr

Manuscript submitted October 21, 2014.

Article published online March 12, 2015

on the magnetic and magnetocaloric properties of lightly doped $\text{La}_{1-x}\text{Bi}_x\text{MnO}_3$ ($x = 0.01, 0.03, 0.06, 0.1,$ and 0.2) compounds has been investigated in detail.

II. EXPERIMENTAL

The polycrystalline samples $\text{La}_{1-x}\text{Bi}_x\text{MnO}_3$ ($x = 0.01, 0.03, 0.06, 0.1,$ and 0.2) were prepared by a conventional solid-state reaction method using high-purity oxide powders of La_2O_3 , Bi_2O_3 , and MnO . First, the powders were mixed in a stoichiometric ratio and ground thoroughly. Then, the mixed powders were calcined in air at 1073 K (800 °C) for 12 hours. After the samples were ground and shaped by a press, they were sintered at 1473 K (1200 °C) for 24 hours in air. The samples were cooled to room temperature at a cooling rate of 276 K/min (3 °C/min). The structural characterizations were performed using X-ray powder diffraction (Cu K_α). The grain structures were observed using a LEO-EVO-40 scanning electron microscope (SEM). The magnetic measurements were performed using a Q-3398 (Cryogenic) magnetometer in a temperature range from 5 K to 300 K (−268 °C to 27 °C), and a maximum magnetic field of 7 T was applied. The magnetic entropy, which is associated with the magnetocaloric effect, was calculated from the isothermal

magnetization curves under the influence of various magnetic fields.

III. RESULTS AND DISCUSSION

Figure 1 shows the X-ray diagrams of the $\text{La}_{1-x}\text{Bi}_x\text{MnO}_3$ ($x = 0.01, 0.03, 0.06, 0.1,$ and 0.2) samples. The results of the X-ray diffraction indicate that the substitution of La by Bi does not produce any significant structural change. As seen in Figure 1, only the diffraction lines of the orthorhombic perovskite are obtained which means that all the samples have a single phase of orthorhombic symmetry. The results are in agreement with the literature.^[12,18] Based on the XRD pattern, the unit cell parameters were calculated for $\text{La}_{1-x}\text{Bi}_x\text{MnO}_3$ ($x = 0.01, 0.03, 0.06, 0.1,$ and 0.2) samples. The results are given in Table I. From X-ray patterns, a distinct doublet diffraction line was observed at just above $2\theta = 30$ deg. Ogawa *et al.*^[12] and Zhang *et al.*^[17] have concluded that this doublet diffraction peak indicates a transformation from the cubic lattice to an orthorhombic or rhombohedral lattice. According to the Goldschmidt rule,^[7] the ideal perovskite cubic lattice depends on the tolerance factor (t) defined as $R_A + R_O = t\sqrt{2}(R_B + R_O)$. The limiting values for the tolerance factor have been determined through experiments. For example, Hines *et al.*^[24] suggested that the perovskite structure forms an ideal cubic lattice if $0.9 < t < 1$. In the range of $0.8 < t < 0.9$, it transforms to a rhombohedral or an orthorhombic lattice. As given in Table I, the calculated values of t vary from 0.8869 for $x = 0.01$ to 0.8876 for $x = 0.2$. This is another additional evidence of the orthorhombic perovskite structure determined from X-ray diffraction patterns. This result is important to understand the main reason for structural deformation in Bi-doped perovskites. Previous studies have shown that the average size of the A-site cations and the size mismatch at the A-site are two important factors that govern the structural properties of these manganites.^[25] In the case considered here, due to the similar ionic radii of Bi^{3+} (1.17 Å) and La^{3+} (1.16 Å), these two factors are eliminated.

As discussed in previous studies, perovskites that have orthorhombic structure generally exhibit larger lattice distortion. In the case of $\text{La}_{1-x}\text{Bi}_x\text{MnO}_3$, the samples show an additional lattice distortion due to the Mn^{3+} ion which is called as Jahn–Teller (J–T) distortion.^[26] When the lattice has predominantly Mn^{3+} ions, then one can observe a cooperative static J–T effect with a

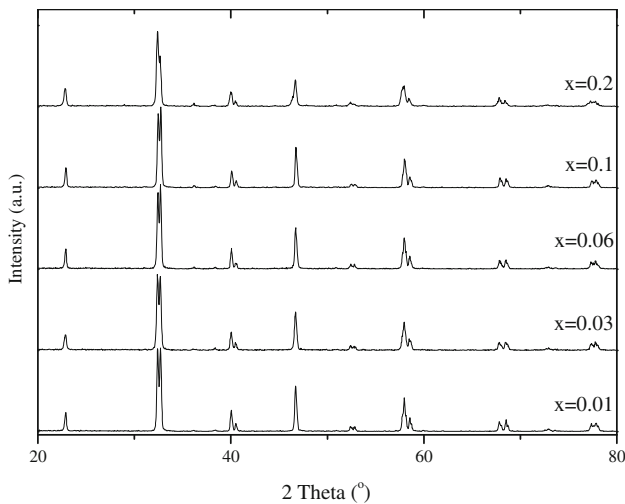


Fig. 1—X-ray diffraction patterns of the $\text{La}_{1-x}\text{Bi}_x\text{MnO}_3$ ($x = 0.01, 0.03, 0.06, 0.1,$ and 0.2) compounds at room temperature.

Table I. Lattice Constants and Other Selected Parameters for $\text{La}_{1-x}\text{Bi}_x\text{MnO}_3$ ($x = 0.01, 0.03, 0.06, 0.1,$ and 0.2) Compounds

Sample	Cell Dimensions (Å)			V (Å ³)	t
	a	b	c		
$\text{La}_{0.99}\text{Bi}_{0.01}\text{MnO}_3$	7.743	5.543	5.490	235.5	0.8869
$\text{La}_{0.97}\text{Bi}_{0.03}\text{MnO}_3$	7.746	5.542	5.491	235.7	0.8870
$\text{La}_{0.94}\text{Bi}_{0.06}\text{MnO}_3$	7.751	5.546	5.492	236.1	0.8871
$\text{La}_{0.9}\text{Bi}_{0.1}\text{MnO}_3$	7.760	5.548	5.493	236.5	0.8872
$\text{La}_{0.8}\text{Bi}_{0.2}\text{MnO}_3$	7.768	5.538	5.496	236.4	0.8876

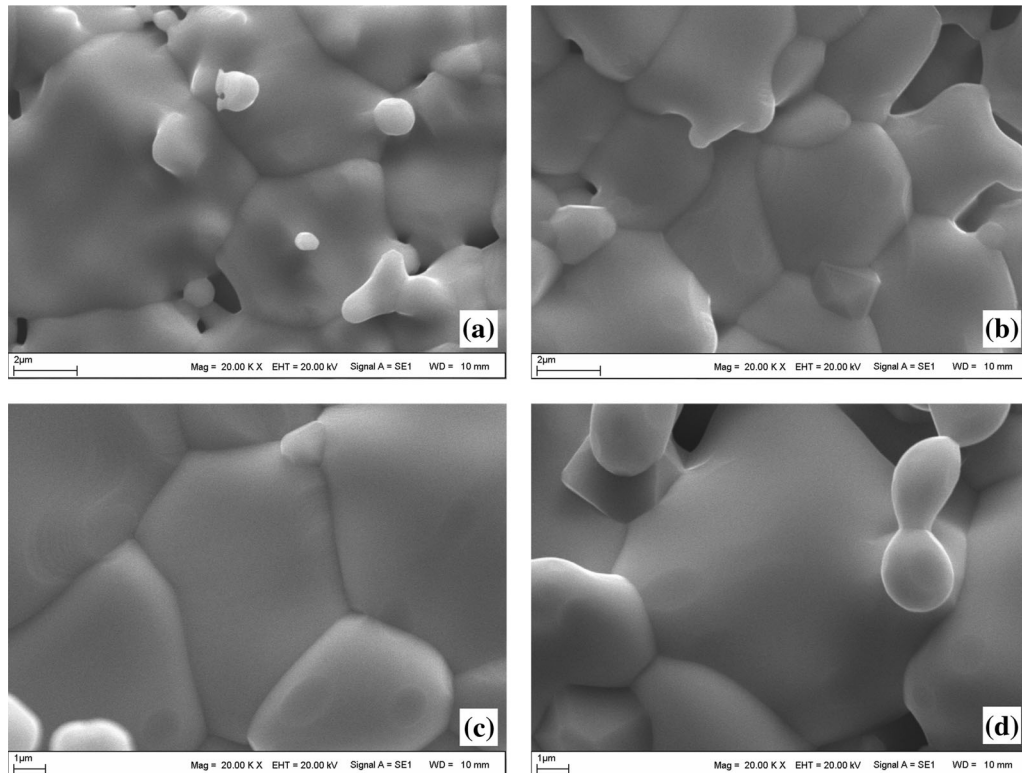


Fig. 2—The SEM photographs of $\text{La}_{1-x}\text{Bi}_x\text{MnO}_3$ compounds with magnification of 20,000, (a) $x = 0.01$, (b) $x = 0.03$, (c) $x = 0.1$, and (d) $x = 0.2$ samples.

permanent distortion of the lattice structure. In present samples, experimentally observed X-ray diffraction results, a distinct doublet diffraction line in X-ray patterns, and values of tolerance factor (vary from 0.8869 for $x = 0.01$ to 0.8876 for $x = 0.2$) all indicate a distorted orthorhombic symmetry. In addition, the existence of predominant Mn^{3+} ions indicates strong J–T distortion in the samples. The results are in agreement with the previous diffuse scattering analysis results which directly measures J–T distortions in other magnetocaloric materials.^[27] Both the above-mentioned J–T effect and the polarized $6s^2$ lone-pair character of Bi^{3+} ^[28] could cause considerable structural distortion in the Bi-doped manganites. It is known that the J–T effect of Mn^{3+} ions derives from having one electron in the e_g band with two-fold degeneracy. The orbital degeneracy is easily lifted by the local deformation of the MnO_6 octahedra (J–T effect), favoring the occupation of the dz^2 and $dx^2 - y^2$ orbitals. In this case, J–T distortion produces a macroscopic lattice strain by compressing the c -axis and expanding the ab plane.^[10,12,17] It has been shown that, due to the $6s^2$ lone-pair character of Bi^{3+} , the Bi–O bond is shorter than the La–O bond, despite the similar ionic radii of the Bi^{3+} and La^{3+} ions.^[29] This can be interpreted as arising from the rather covalent character of the Bi–O bonds. The electronegativity of Bi enhances the hybridization between $6s$ of the Bi^{3+} orbitals and $2p$ of the O^{2-} orbitals and can produce a local distortion. The measured 159° deg of the Mn–O–Mn bond angle for the

Bi-doped sample,^[30] which is smaller than that of an undoped sample, is evidence of local distortion.

Figures 2(a) through (d) show typical SEM micrographs for $x = 0.01$, 0.03 , 0.1 , and 0.2 samples with a magnification of 20,000. All the SEM images reflect a smooth polycrystalline structure with the average grain size between 2 and $12 \mu\text{m}$, and the grains were dispersed randomly in all samples. It is clearly seen from SEM images that the average grain size slightly increases with increasing Bi content. The variation of grain size with increasing Bi content is in agreement with the results given in our previous study.^[11] In this study, it has been demonstrated that Bi doping promotes grain growth and good sample crystalline structure due to the low melting temperature of Bi in $\text{La}_{0.67-x}\text{Bi}_x\text{Ca}_{0.33}\text{MnO}_3$ compounds.

Figure 3 shows the temperature dependence of the magnetization of the $\text{La}_{1-x}\text{Bi}_x\text{MnO}_3$ samples for different Bi doping levels ($x = 0.01$, 0.03 , 0.06 , 0.1 , and 0.2). The data were taken in a wide range of temperature [from 5 K to 300 K (-268°C to 27°C)] and an applied field of 0.1 T. It can be clearly seen that a transition from ferromagnetic to paramagnetic phase occurs in all the samples near the Curie temperature. It is generally known that the variation of magnetization curve at transition temperature gives a clue about the nature of phase transition. The magnetization curves reveal that the samples for $x = 0.01$, 0.03 , 0.06 , and 0.1 exhibit a sharp ferromagnetic–paramagnetic transition at their transition temperature which is a characteristic of the

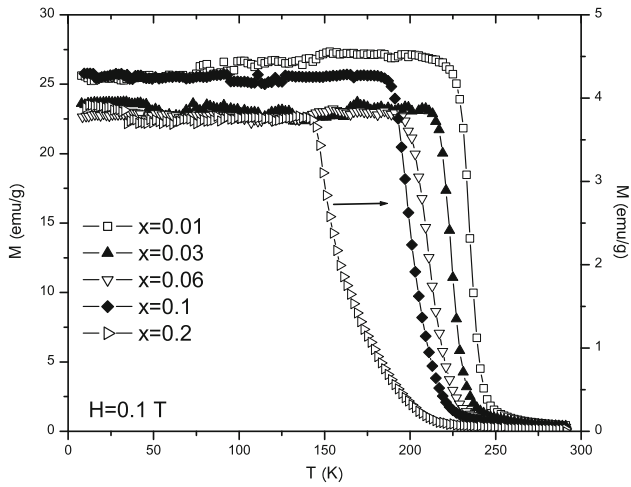


Fig. 3—Temperature dependence of the magnetization for $\text{La}_{1-x}\text{Bi}_x\text{MnO}_3$ ($x = 0.01, 0.03, 0.06, 0.1,$ and 0.2) compounds, measured for 0.1 T magnetic field.

first-order phase transition. However, the sharpness of the transition from ferromagnetic to paramagnetic phase decreases for $x = 0.2$ sample which indicates the transformation of nature of phase transition from first order to second order. The Curie temperature, T_c , can be defined as the temperature of the maximum value for $|dM/dT|$. The Curie temperatures were measured to be $234 \text{ K}, 224 \text{ K}, 209 \text{ K}, 198 \text{ K},$ and 149 K ($-39^\circ\text{C}, -49^\circ\text{C}, -64^\circ\text{C}, -75^\circ\text{C},$ and -124°C) for $x = 0.01, 0.03, 0.06, 0.1,$ and 0.2 , respectively.

Figures 4(a) through (d) show the isothermal magnetization curves as a function of applied magnetic field at different temperatures for $\text{La}_{1-x}\text{Bi}_x\text{MnO}_3$ ($x = 0.01, 0.03, 0.06,$ and 0.2) samples. For all samples, after the field is turned on, the magnetization increases as the field aligns the ferromagnetic phase in the samples. At low temperatures, the magnetization curves exhibit typical ferromagnetic behavior and approaching saturation at high fields. At higher temperatures, the magnetization curves completely become linear with magnetic field

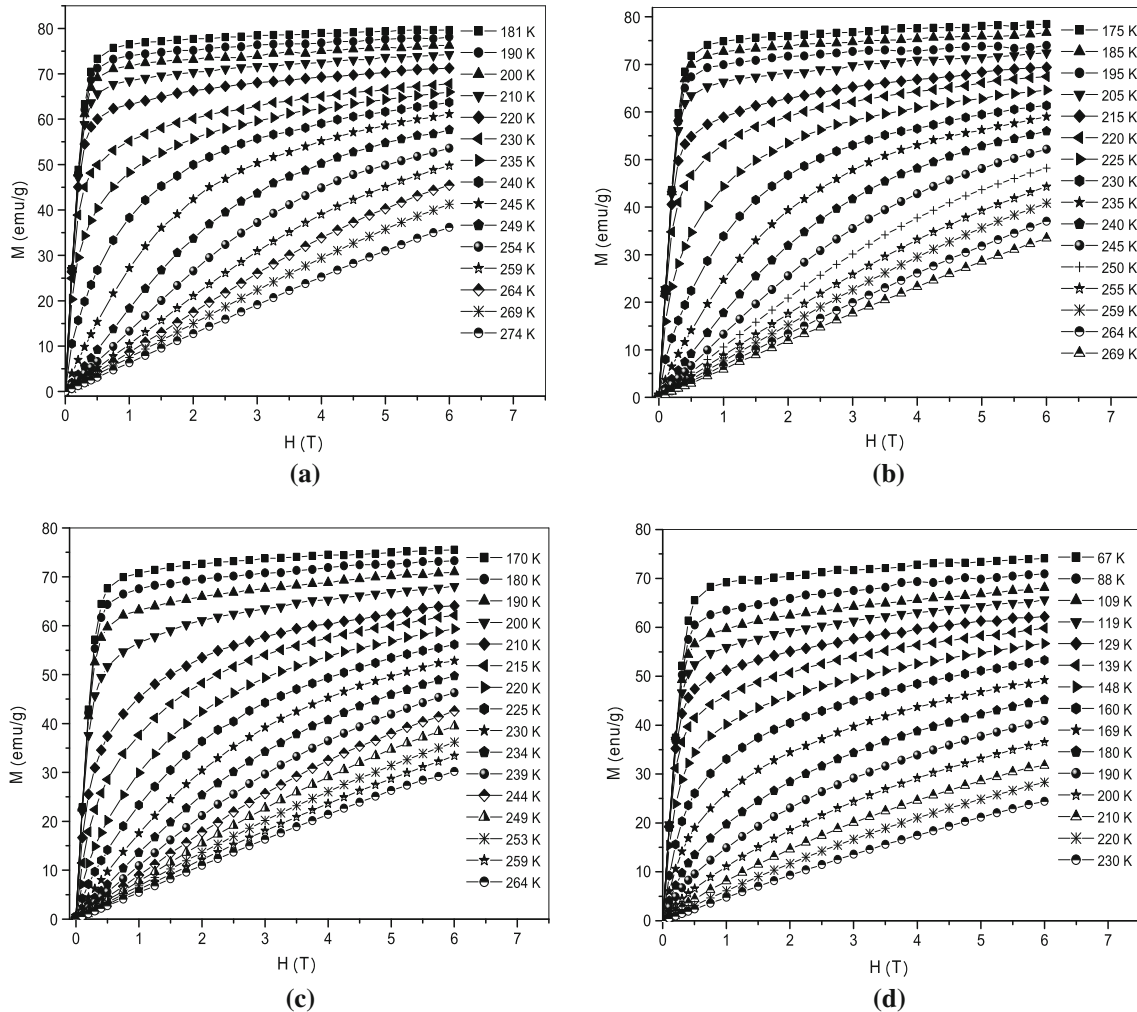


Fig. 4—Isothermal magnetization curves at various temperatures for (a) $x = 0.01,$ (b) $x = 0.03,$ (c) $x = 0.06,$ and (d) $x = 0.2$ samples.

which resembling the paramagnetic phase. The saturation magnetizations were determined to be 89, 87, 85, and 80 emu/g for $x = 0.01, 0.03, 0.06,$ and $0.2,$ respectively. The decrease of saturation magnetization with increasing Bi content is an evidence of ferromagnetic dilution in Bi-doped samples.

Figure 5 shows the variation of the Curie temperature and saturation magnetization as a function of Bi content (x). As can be seen, both the Curie temperature and saturation magnetization decrease with increasing Bi content. Although there are many studies on Bi-doped $\text{La}_{1-x}\text{Bi}_x\text{MnO}_3$ manganites, the variation of Curie temperature with Bi content is not clear. For example, the Curie temperature for $\text{La}_{0.8}\text{Bi}_{0.2}\text{MnO}_3$ sample was determined as 167 K (-106°C) in Reference 8, 139 K (-134°C) in Reference 11, 138 K (-135°C) in References 6, 12, 143 K (-130°C) in Reference 7, and finally 149 K (-124°C) in our study. Although the sample compositions are same in all the studies, the Curie temperatures are very different from each other. The reason for this difference in Curie temperature is still not clear. Ogawa *et al.*^[12,18] measured the Curie temperature as a function of Bi content in $\text{La}_{1-x}\text{Bi}_x\text{MnO}_3$, and they found that the Curie temperature decreases linearly with increasing Bi content from 153 K (-120°C) for $x = 0.1$ to 115 K (-158°C) for $x = 0.4$. It is clearly seen in our study that the variation of Curie temperature with increasing Bi content shows the same trend with results given in References 12 and 18. The decrease of Curie temperature with increasing Bi content is a clear evidence of weakening of ferromagnetic interactions. The decrease in saturation magnetization (Figure 5) with increasing Bi content is another evidence of ferromagnetic dilution.

It is generally known that, in mixed-valence manganites, the ferromagnetism and the metallic character of the samples are generally explained by the DE interaction between the Mn^{3+} and Mn^{4+} ions. Zhang *et al.*^[17] have demonstrated that the electronic state of the Mn ions in the Bi-doped compound proves that the trivalent state is maintained after trivalent Bi^{3+} ions are doped into the structure. In this case, the observed ferromag-

netic properties and the FM–PM phase transition in the sample must be explained without the existence of the double-exchange interaction, due to the absence of Mn^{4+} . The only way to explain the ferromagnetism in this system is the super-exchange interaction between Mn^{3+} ions. Although superexchange between Mn^{3+} ions exhibits antiferromagnetic ordering when the $\text{Mn}^{3+}\text{-O-Mn}^{3+}$ bond angle is 180 deg, ferromagnetic ordering can be obtained when the bond angle of $\text{Mn}^{3+}\text{-O-Mn}^{3+}$ is reduced to lower than 180 deg with a higher lattice distortion.

As discussed above, J–T distortion and the highly polarizable Bi^{3+} $6s^2$ lone-pair character play an important role for exhibiting ferromagnetism.^[26–30] As a result of J–T distortion and the $6s^2$ lone-pair character of Bi^{3+} , the Mn^{3+} ions with ordered dz^2 orbitals and ordered $dx^2 - y^2$ orbitals are positioned in a chessboard pattern, and the axes of the dz^2 orbitals are oriented along the b-axis. The orbitals in the neighboring (a, c) plane are oriented in such a way that there is an overlap of the half-filled and empty e_g orbitals of the Mn^{3+} ions along all the Mn–O–Mn directions. In this case, at each Mn^{3+} ion, the conditions are satisfied for the ferromagnetic $\text{Mn}^{3+}\text{-O-Mn}^{3+}$ exchange interaction.^[26] Consequently, ferromagnetism in the $\text{La}_{1-x}\text{Bi}_x\text{MnO}_3$ ($x = 0.01, 0.03, 0.06, 0.1,$ and 0.2) compounds are considered to be caused by the specific ordering of the dz^2 orbitals of the Mn^{3+} ions. Khomchenko *et al.*^[15] and Atou^[21] have concluded that two-thirds of the total value of the exchange coupling is positive and that the resulting structure is ferromagnetic. Ogawa *et al.*^[12] have concluded that the decrease of saturation magnetization with increasing Bi content could be understood by considering J–T distortion. In very low concentration rates, the magnetic ordering of the local magnetic moment of Mn^{3+} ions seems to be nearly realized because the saturation magnetization has maximum value (89 emu/g for $x = 0.01$). At that concentration rates, J–T distortion is relatively relaxed. For the further concentration rates, the decrease in saturation magnetization could be due to the increasing J–T distortion which affects the ferromagnetic ordering of magnetic moments of Mn^{3+} ions.

The magnetic entropy, which is associated with the magnetocaloric effect, can be calculated from the isothermal magnetization curves (as given in Figure 4) under the influence of a magnetic field. According to the classical thermodynamic theory, the magnetic entropy change ΔS_m produced by the variation of a magnetic field from 0 to H_{\max} is given by

$$\Delta S_m(T, H) = \int_0^{H_{\max}} \left(\frac{\partial M}{\partial T} \right)_H dH. \quad [1]$$

To evaluate the magnetic entropy change ΔS_m , one must make a numerical approximation to the integral in Eq. [1]. The usual method is to use the isothermal magnetization measurements at a small, discrete field interval. In this case, $|\Delta S_m|$ can be approximated from Eq. [1] by

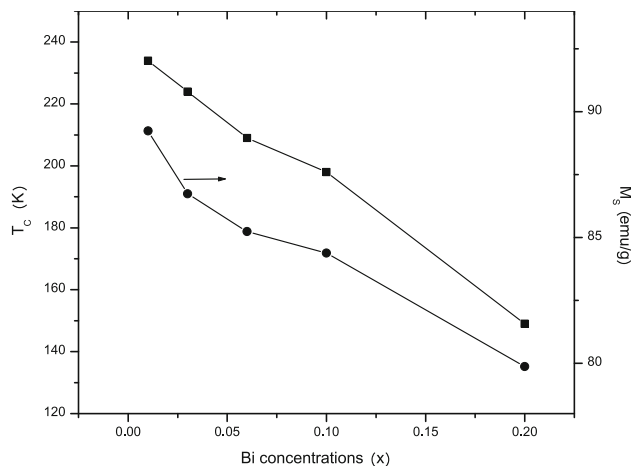


Fig. 5—The variation of Curie temperature and saturation magnetization as a function of Bi concentration.

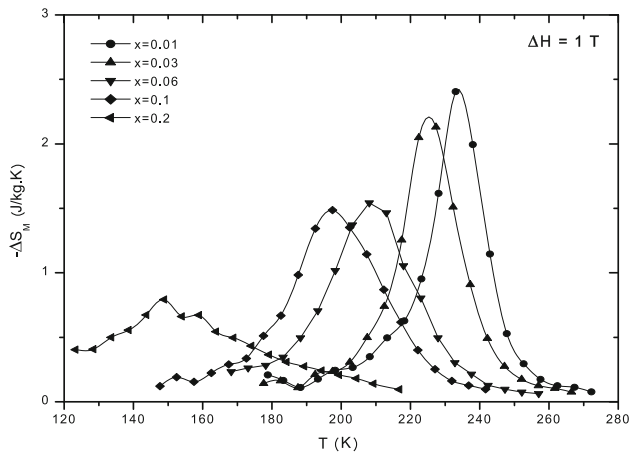


Fig. 6—The temperature dependence of the magnetic entropy change ($|\Delta S_m|$) for the $\text{La}_{1-x}\text{Bi}_x\text{MnO}_3$ ($x = 0.01, 0.03, 0.06, 0.1,$ and 0.2) compounds at 0.1 T magnetic field change.

$$|\Delta S_m| = \sum_i \frac{M_i - M_{i+1}}{T_{i+1} - T_i} \Delta H, \quad [2]$$

where M_i and M_{i+1} are the experimental values of the magnetization at T_i and T_{i+1} , respectively, under an applied magnetic field H_i . Using Eq. [2], by measuring the M - H curve at various temperatures, one can calculate the magnetic entropy change at various magnetic fields.

Figure 6 shows the magnetic entropy change as a function of temperature of $\text{La}_{1-x}\text{Bi}_x\text{MnO}_3$ ($x = 0.01, 0.03, 0.06, 0.1,$ and 0.2) compounds at 1 T magnetic field. For all the samples, the magnetic entropy change exhibits a peak in the vicinity of Curie temperature. The peak temperatures shift to lower temperature with increasing Bi content. The peak value of $|\Delta S_m|$ was determined to decrease from 2.42 J/kg K for $x = 0.01$ to 0.79 J/kg K for $x = 0.2$ sample. It is clear that measured magnetic entropy change values are comparable with magnetic entropy change of various manganites. For example, $|\Delta S_m| = 1.58$ J/kg K at a 1 T magnetic field for $\text{La}_{0.94}\text{Bi}_{0.06}\text{MnO}_3$ is nearly identical to the values of 1.55 J/kg K for $\text{La}_{0.67}\text{Sr}_{0.33}\text{MnO}_3$ ^[31] and 1.6 J/kg K for $\text{La}_{0.67}\text{Ba}_{0.33}\text{MnO}_3$ ^[32] at the same magnetic field. The refrigeration capacity (RC) was calculated from the direct product of the maximum entropy change and the full width at half maximum of the peak ($= \Delta S_m \delta T_{\text{FWHM}}$). The calculated values are 42.19, 42.85, 44.86, 46.04, and 39.50 J/kg at 1T magnetic field change for the $\text{La}_{1-x}\text{Bi}_x\text{MnO}_3$ ($x = 0.01, 0.03, 0.06, 0.1,$ and 0.2) samples, respectively.

It is generally known that the value of magnetic entropy change in manganites is closely related with saturation magnetization and nature of phase transition which can be investigated using Landau theory.^[33] The magnetic free energy $F(M, T)$ can be expanded as a Landau expansion in the powers of the magnetization M , neglecting higher order contributions, as

$$F(M, T) = \frac{c_1(T)}{2} M^2 + \frac{c_3(T)}{4} M^4 - MH. \quad [3]$$

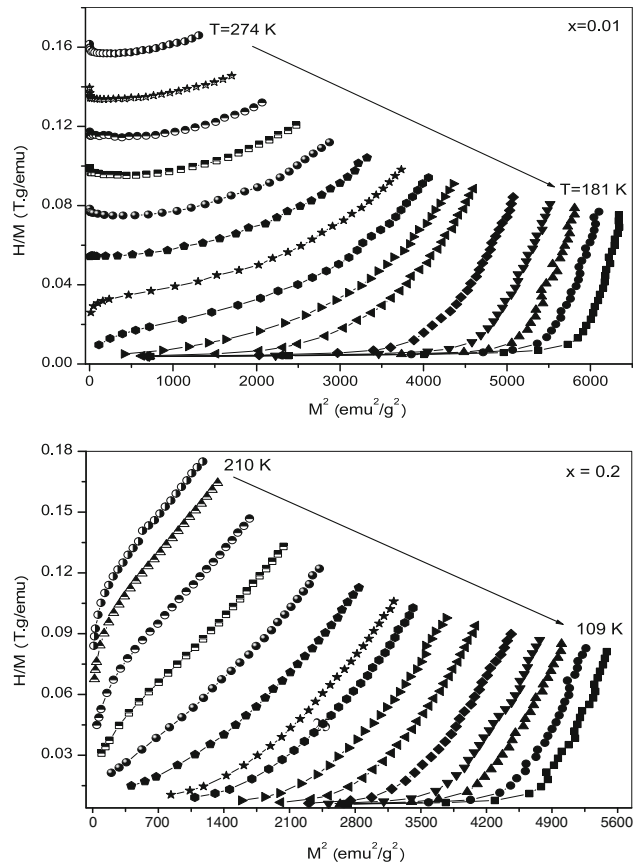


Fig. 7—Arrott plots for the $\text{La}_{1-x}\text{Bi}_x\text{MnO}_3$ ($x = 0.01$ and 0.2) compounds at various temperatures.

Here, $c_1(T)$ and $c_3(T)$ are termed the Landau coefficients, and the sign of the $c_3(T)$ determines the type of the magnetic phase transition. A first-order phase transition is expected in the case $c_3(T) < 0$, and a second-order phase transition in the case $c_3(T) > 0$.^[33] From the condition of equilibrium $\partial F(M, T)/\partial M = 0$, we obtain

$$H = c_1(T) M + c_3(T) M^3 \quad [4a]$$

$$\frac{H}{M} = c_1(T) + c_3(T) M^2. \quad [4b]$$

By plotting H/M vs M^2 in the critical region, which is called an Arrott plot, the slope of the resulting curves denotes whether a magnetic transition is of first order or second order. It can be deduced that, if all the curves have a positive slope, the magnetic transition is second order. On the other hand, if several of the curves show a negative slope at some point, then the magnetic transition is first order. It has been concluded that the slope of the Arrott plots is not a universal tool for determining the type of the phase transition because the slope is positive not only in the case of second-order transition but also in the case of first-order transition when T is inside the transition region.^[33]

Figure 7 shows the Arrott plots of the $\text{La}_{1-x}\text{Bi}_x\text{MnO}_3$ for $x = 0.01$ and 0.2 samples. The negative slope of the plots for $x = 0.01$ sample clearly shows the first-order nature of the magnetic phase transition from ferromagnetic to paramagnetic. The negative slopes (which they were not given here) were observed up to $x = 0.1$ sample. For higher doping concentration ($x = 0.2$), the nearly positive slope of H/M vs M^2 curve reveals that the magnetic phase transition has changed to second order. The Landau coefficient $c_3(T)$ could be determined by fitting Eq. [4a] to the magnetic field H against the magnetization M (Figure 4) or fitting Eq. [4b] to the Arrott plot (Figure 7). Our calculations have shown that for lower concentration rates, the $c_3(T)$ coefficients ($-2 \times 10^{-5} \text{ T gr}^3/\text{emu}^3$ for $x = 0.01$, $-3.3 \times 10^{-4} \text{ T gr}^3/\text{emu}^3$ for $x = 0.03$ and $-1.8 \times 10^{-4} \text{ T gr}^3/\text{emu}^3$ for $x = 0.1$) are negative near the Curie temperature. According to the theory described above, a negative value of $c_3(T)$ suggests that the phase transitions for $\text{La}_{0.99}\text{Bi}_{0.01}\text{MnO}_3$, $\text{La}_{0.97}\text{Bi}_{0.03}\text{MnO}_3$, and $\text{La}_{0.9}\text{Bi}_{0.1}\text{MnO}_3$ samples are first order. Unlike the lower concentration rates, the positive value of $c_3(T)$ coefficient ($5 \times 10^{-5} \text{ T gr}^3/\text{emu}^3$) for $x = 0.2$ sample is another evidence of nature of phase transition changing from first order to second order for higher order Bi concentration. The considerable decrease of $|\Delta S_m|$ for increasing Bi content (from 2.42 J/kg K for $x = 0.01$ to 0.79 J/kg K for $x = 0.2$ sample at 1 T magnetic field) could be due to the nature of phase transition changing from first order to second order.

IV. CONCLUSIONS

In this study, magnetocaloric properties of $\text{La}_{1-x}\text{Bi}_x\text{MnO}_3$ ($x = 0.01, 0.03, 0.06, 0.1,$ and 0.2) samples were investigated in detail. X-ray diffraction measurement showed that the sample crystallized exclusively in the orthorhombic perovskite structure. A distinct doublet diffraction line observed at just above $2\theta = 30$ deg has concluded due to a transition from the ideal cubic lattice to a distorted orthorhombic lattice. Such a considerable distortion in lattice symmetry was attributed to the J-T effect and $6s^2$ lone-pair character of the Bi^{3+} ions. The Curie temperatures were measured to be $234 \text{ K}, 224 \text{ K}, 209 \text{ K}, 198 \text{ K},$ and 149 K ($-39 \text{ }^\circ\text{C}, -49 \text{ }^\circ\text{C}, -64 \text{ }^\circ\text{C}, -75 \text{ }^\circ\text{C},$ and $-124 \text{ }^\circ\text{C}$) and the saturation magnetizations were determined to be $89, 88, 85, 84,$ and 80 emu/g for $x = 0.01, 0.03, 0.06, 0.1,$ and 0.2 , respectively. The observed ferromagnetism in $\text{La}_{1-x}\text{Bi}_x\text{MnO}_3$ samples was interpreted by the ferromagnetic–superexchange interaction along the Mn^{3+} -O-Mn $^{3+}$ bonds. The magnetic entropy change ($|\Delta S_m|$) was determined to decrease from 2.42 J/kg K for $x = 0.01$ to 0.79 J/kg K for $x = 0.2$ sample. The decrease in magnetic entropy change was attributed to the decrease in saturation magnetization and a change of the nature of the phase transition from first order to second order with increasing Bi content.

ACKNOWLEDGMENTS

This work was supported by Inonu University with Project Number 2012/37.

REFERENCES

1. V.K. Pecharsky and K.A. Gschneidner: *Phys. Rev. Lett.*, 1997, vol. 78, pp. 4494–97.
2. Z.M. Wang, G. Ni, Q.Y. Xu, H. Song, and Y.W. Du: *J. Appl. Phys.*, 2001, vol. 90, pp. 5689–91.
3. A.P. Ramirez: *J. Phys.: Condens. Matter*, 1997, vol. 9, pp. 8171–99.
4. V.S. Kolat, T. Izgi, A.O. Kaya, N. Bayri, H. Gencer, and S. Atalay: *J. Magn. Magn. Mater.*, 2010, vol. 322, pp. 427–33.
5. C. Zener: *Phys. Rev.*, 1951, vol. 82, pp. 403–05.
6. H. Chiba, T. Atou, and Y. Syono: *J. Solid State Chem.*, 1997, vol. 132, pp. 139–43.
7. F. Sugawara, S. Iiida, Y. Syono, and S.I. Akimoto: *J. Phys. Soc. Jpn.*, 1968, vol. 25, pp. 1553–58.
8. I.O. Troyanchuk, O.S. Mantyskaya, and A.N. Chobot: *Phys. Solid State*, 2002, vol. 44, pp. 2266–70.
9. A. Moreira dos Santos, A.K. Cheetham, T. Atou, Y. Syono, Y. Yamaguchi, K. Ohoyama, H. Chiba, and C.N.R. Rao: *Phys. Rev. B*, 2002, vol. 66, p. 064425 (1–4).
10. Y.D. Zhao, J. Park, R.J. Jung, H.J. Noh, and S.J. Oh: *J. Magn. Magn. Mater.*, 2004, vol. 280, pp. 404–11.
11. H. Gencer, S. Atalay, H.I. Adiguzel, and V.S. Kolat: *Phys. B*, 2005, vol. 357, pp. 326–33.
12. T. Ogawa, H. Shindo, H. Takeuchi, and Y. Koizumi: *Jpn. J. Appl. Phys.*, 2006, vol. 45, pp. 8666–72.
13. V. Dayal and V.P. Kumar: *J. Magn. Magn. Mater.*, 2014, vol. 361, pp. 212–18.
14. S. Atalay, V.S. Kolat, H. Gencer, and H.I. Adiguzel: *J. Magn. Magn. Mater.*, 2006, vol. 305, pp. 452–56.
15. V.A. Khomchenko, I.O. Troyanchuk, O.S. Mantyskaya, M. Tovar, and H. Szymczak: *J. Exp. Theor. Phys.*, 2006, vol. 103, pp. 54–59.
16. H. Gencer and S. Atalay: *Int. J. Mod. Phys. B*, 2005, vol. 19, pp. 4115–23.
17. H.G. Zhang, Y.T. Li, X.G. Dong, Q.T. Hou, Y.C. Huang, H. Liu, and Q. Li: *J. Phys. Conf. Ser.*, 2013, vol. 430, p. 012072 (1–4).
18. T. Ogawa, A. Sandhu, M. Chiba, H. Takeuchi, and Y. Koizumi: *J. Magn. Magn. Mater.*, 2005, vols. 290–291, pp. 933–36.
19. T. Izgi, V.S. Kolat, N. Bayri, H. Gencer, and S. Atalay: *J. Magn. Magn. Mater.*, 2014, vol. 372, pp. 112–16.
20. J.L. Garcia-Munoz, C. Frontera, M.A.G. Aranda, A. Llobet, and C. Ritter: *Phys. Rev. B*, 2001, vol. 63, p. 064415 (1–4).
21. T. Atou, H. Chiba, K. Ohoyama, Y. Yamaguchi, and Y. Syono: *J. Solid State Chem.*, 1999, vol. 145, pp. 639–42.
22. C.H. Yang, T.Y. Koo, S.H. Lee, C. Song, K.B. Lee, and Y.H. Jeong: *Europhys. Lett.*, 2006, vol. 74, pp. 348–54.
23. Z.H. Chi, C.J. Xiao, S.M. Feng, F.Y. Li, C.Q. Jin, X.H. Wang, R.Z. Chen, and L.Y. Li: *J. Appl. Phys.*, 2005, vol. 98, pp. 103519–24.
24. R.I. Hines: Ph.D., University of Bristol, 1997.
25. H.Y. Hwang, S.E. Cheong, P.G. Radaelli, M. Marezio, and B. Batlogg: *Phys. Rev. Lett.*, 1995, vol. 75, pp. 914–17.
26. I.O. Troyanchuk, N.V. Kasper, O.S. Mantyskaya, and S.N. Pastushook: *J. Exp. Theor. Phys.*, 1994, vol. 78, pp. 212–15.
27. R.I. Barabash, O.M. Barabash, E.A. Karapetrova, and M.E. Manley: *Appl. Phys. Lett.*, 2014, vol. 104, p. 241905 (1–4).
28. R. Seshadri and N.A. Hill: *Chem. Mater.*, 2001, vol. 13, pp. 2892–99.
29. L. Righi, M. Amboage, J. Gutierrez, J.M. Barandiaran, L.F. Barquin, and M.T.F. Diaz: *Phys. B*, 2000, vols. 276–278, pp. 718–19.
30. J.M. Barandiaran, J. Gutierrez, J.R. Fernandez, M. Amboage, and L. Righi: *Phys. B*, 2004, vol. 343, pp. 79–83.
31. A. Rostamnejadi, M. Venkatesam, P. Kaneli, H. Salamati, and J.M.D. Coey: *J. Magn. Magn. Mater.*, 2011, vol. 323, pp. 2214–18.
32. M.H. Phan, T.L. Phan, S.C. Yu, K.W. Lee, and S.H. Park: *J. Korean Phys. Soc.*, 2004, vol. 45, pp. 664–67.
33. V.K. Pecharsky and K.A. Gschneidner: *J. Magn. Magn. Mater.*, 1999, vol. 200, pp. 44–46.